We are IntechOpen,
the world's leading publisher of Open Access books
Built by scientists, for scientists

4,800
Open access books available

122,000
International authors and editors

135M
Downloads

154
Countries delivered to

Our authors are among the

TOP 1%
most cited scientists

12.2%
Contributors from top 500 universities

CLARIVATE ANALYTICS
BOOK CITATION INDEX
INDEXED

WEB OF SCIENCE™

Selection of our books indexed in the Book Citation Index
in Web of Science™ Core Collection (BKCI)

Interested in publishing with us?
Contact book.department@intechopen.com

Identification of Active Faults in Landslide-Prone Regions Using Ground-Penetrating Radar: A Case Study from Bandung, Indonesia

Maman Hermana, Maya Genisa, Luluan A. Lubis and Chow Weng Sum

Abstract

Ground-penetrating radar or georadar is a popular method in engineering and archeology for investigation of objects in shallow subsurface at high resolution. Georadars produce electromagnetic waves which propagate into the subsurface, and its interaction with the dielectric contrast is reflected and recorded in the radargram. It is an environmentally safe and nondestructive method and can be used for monitoring of active faults in the landslide-prone regions. This chapter explains the concept of georadar and its implementation on the detection of the active fault—Lembang fault—located in Bandung, Indonesia. Bandung is a highly populated city with many living around the active fault which poses a high risk of landslides. The Lembang fault was created by tectonic forces during the Pleistocene and has been constantly reactivated by recent volcanic events. It is the largest active fault in West Java, Indonesia, which is located in the midst of a densely populated urban area. A georadar survey using 25 MHz and 50 Hz frequency antenna was conducted to detect the fault in the urban setting. Unix-based seismic software was used to process the electromagnetic signals. The results showed that the georadar method was successful in identifying the active fault with clear imaging of the subsurface structures and basement of the region.

Keywords: fault, georadar, electromagnetic wave, wave propagation, radargram

1. Introduction

Georadar method is commonly used for engineering and archeology since 1980 [1]. The target of this method usually is to image shallow/near surface. The method promises to give a better resolution and accuracy specially to detect the fault system and other subsurface structures in detail. Georadar is based on electromagnetic wave which detects the contrast of dielectric properties of medium. Due to the high frequency, georadar is able to effectively identify the shallow objects with a high resolution.

The instrument of georadar is equipped with transmitter and receiver antennas which has the ability to transmit and receive electromagnetic wave into and from

the earth at certain frequency ranges. Data are recorded as time series in two-way time (TWT) manner which after processing can be converted into depth domain by adding the velocity model during processing. **Figure 1** shows the georadar instrument and example of recorded data.

Due to the ability of detecting shallow object with high resolution, georadar has been applied in many fields with various objectives. Georadar is able to distinguish two different objects based on different electrical properties; hence, georadar are commonly used in various field such as environment study, mining, ground water, ancient artifact, and others. Not only able to detect the electrical properties contrast of material, but also georadar is able to detect the subsurface structure like faults and folds. Hence, the application of georadar for detecting the subsurface structures and monitoring of active faults for mitigation purposes are promising, especially for unstable area in the urban/suburban area with high population where other active source is prohibited.

The exact location of an active fault in urban area is very important to be known for the mitigation purposes. Hence, the potential landslide due to the unstable structure of this area can be warned early to avoid serious hazard or disaster. Many techniques have been used to monitor the stability and mitigate the potential landslide in the area around the active fault which is across the urban area. Nondestructive geophysical methods such as electrical method and electromagnetic method are commonly selected for the investigation and evaluation of the subsurface structure this area. Geo-penetrating radar (GPR) or georadar method is also a common geophysical method that is applied to understand the bedding subsurface and structure in the high-risk area in such condition.

Lembang fault is an example for active fault across urban area with high population density in Bandung, Indonesia. In this area, there are not less than 8 million people leaving around the Lembang fault. The length of this fault itself is about 29 km from east to west part of Bandung [3] as illustrated in **Figure 2**. Because of the compression system in this area, it is predicted that a huge accumulated energy is concentrated in this fault and potentially can be released any time as an earthquake. The earthquake then is predicted also which leads to trigger the local landslide in this area.

Due to some reasons such as soil stability and environmental concern, techniques such as seismic refraction and seismic reflection that use dynamite explosion as a source, are not allowed. Hence the use of georadar technique for identifying
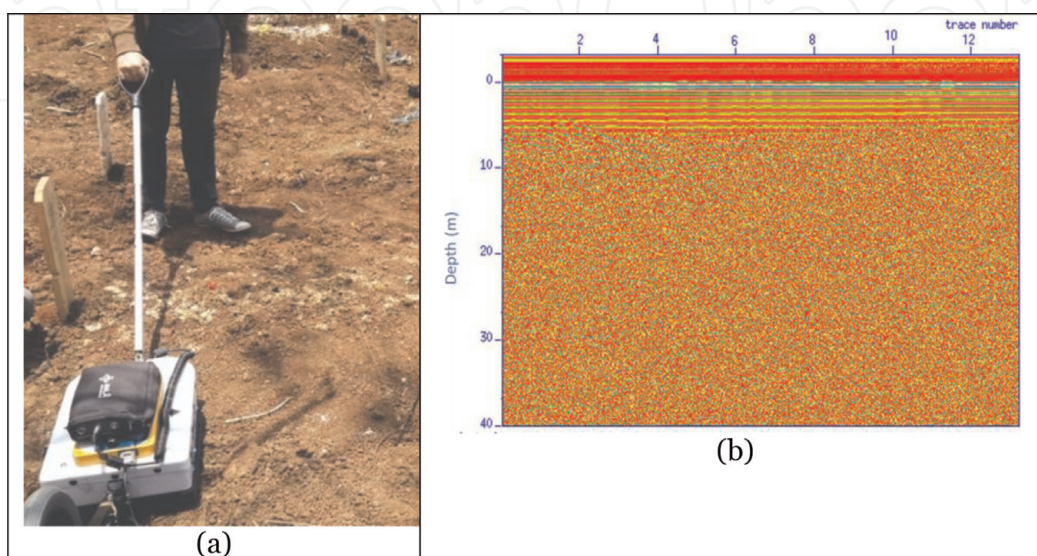

(a)   (b)

Figure 1.
(a) Georadar instrument [2], (b) example of recorded subsurface data.
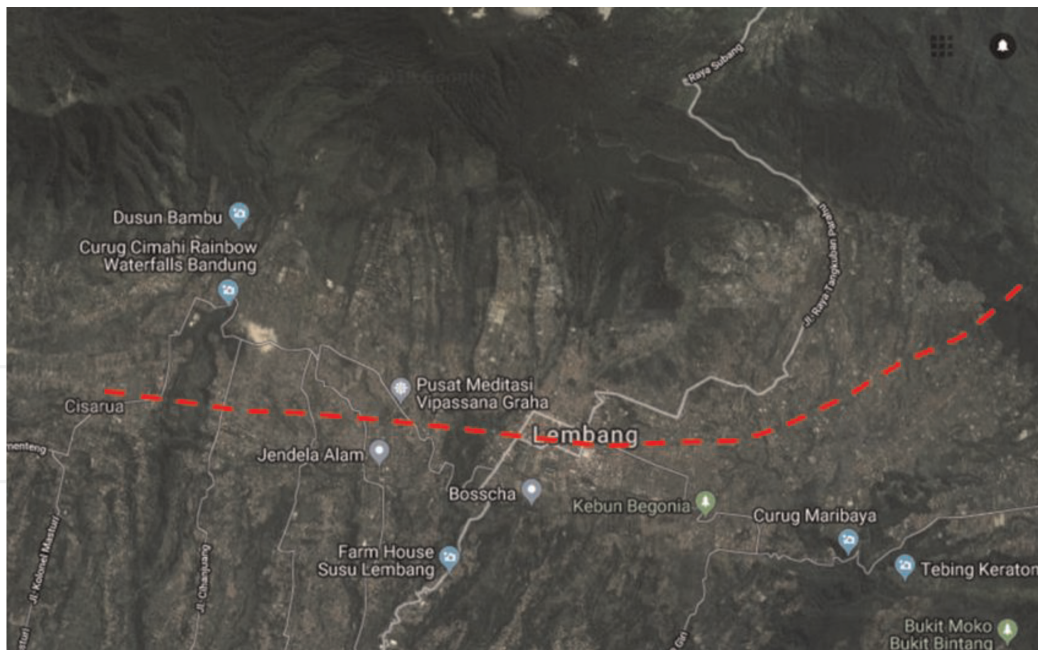
2

Figure 2.
Active fault (Lembang fault) located from west to east part of Bandung.

fault system in this area becomes more significant. This chapter discusses the example of GPR technique for detecting fault in urban area. The background theory of GPR, design survey, and data gathering, processing, and interpretation of GPR data are discussed and applied for detecting an active fault of Lembang fault in Bandung, Indonesia.

2. Background theory

2.1 Georadar wave propagation

Georadar technique is developed based on electromagnetic wave propagation theory. In one dimension (1D), the propagation of electromagnetic wave in z-direction is explained by Maxwell equation:

$$\frac{\partial^2 E}{\partial z^2} = \mu\varepsilon\frac{\partial^2 E}{\partial t^2} \tag{1}$$

The propagation of the electromagnetic wave is perpendicular to the electrical field (E) and magnetic field (H) and controlled by the velocity and attenuation of medium. The properties of medium are also related to the mineral composition and also water saturation of medium. The velocity of wave propagation in the medium depends on the velocity of electromagnetic wave in the vacuum (c = 0.3 m/ns), relative dielectric constant (ε_r), and relative magnetic permeability ($\mu_r = 1$ for nonmagnetic material):

$$V_m = c/\left\{(\varepsilon_r\mu_r/2)\left[(1 + P^2) + 1\right]\right\}^{1/2} \tag{2}$$

where $P = \sigma/\omega\varepsilon$ is an absorption factor and σ is conductivity of medium, $\varpi = 2\pi f$, where f is frequency and $\varepsilon = \varepsilon_r\varepsilon_o$ is vacuum permittivity (8.854×10^{-12} F/m). For the material with low loss, $P \sim 0$, the velocity of georadar is

$$V_m = c/\sqrt{\varepsilon_r} = 0.3/\sqrt{\varepsilon_r}$$

Recording of georadar data is based on the reflection responses of dielectric contrast of medium. If dielectric contrast in the interface between different layers is strong, the reflectors have a strong amplitude in the georadargram. The strength of reflection (reflection coefficient R) is determined by the contrast of velocity and relative dielectric of medium at the boundary. The number of reflected energy is proportional to R:

$$R = \frac{(V_1 - V_2)}{(V_1 + V_2)} \text{ or } R = \frac{\sqrt{\varepsilon_2} - \sqrt{\varepsilon_1}}{\sqrt{\varepsilon_2} - \sqrt{\varepsilon_1}} \tag{3}$$

where v_1 and v_2 are wave velocity of georadar at first and second layers and ε_1 and ε_2 are relative dielectric constant at first and second layers, respectively.

The energy loss during wave propagation is determined by some factors: antenna, transmission between air and soil, reduction due to the configuration or distance between transmitter and receiver, attenuation, and diffraction due to the sharp object. The energy reduction due to the wave propagation between transmitter and receiver is proportional to $1/r^2$, where the r is distance measured between source/antenna and receiver (another antenna), attenuation factor which defend on the dielectric properties of medium, and its magnetic and electrical field itself in the medium. Amplitude will be reduced in the depth of penetration due to the attenuation which is proportional to $1/e$ (about 37%) of initial energy which also called as skin depth. The skin depth depends on soil resistivity. The ratio of two different amplitudes is formulated as

$$E_o/E_x = \exp(-\alpha x) \tag{4}$$

where α is attenuation coefficient

$$\alpha = \omega \left\{ \left(\frac{\mu\varepsilon}{2} \right) \left[\left(1 + \frac{\sigma^2}{\omega^2 \varepsilon^2} \right)^{1/2} - 1 \right] \right\}^{1/2} \tag{5}$$

Loss factor $(P) = \sigma/\omega\epsilon = \tan D$ and skin depth is defined as

$$\delta = 1/\alpha$$

If $D < <1$, $\delta = (2/\sigma)(\varepsilon/\mu)^{1/2}$, the skin depth is formulated:

$$\delta = (5.31\sqrt{\varepsilon_r})/\sigma$$

where σ is an electrical conductivity (mS/m).

In the saturated porous medium, the loss energy is proportional to the conductivity and invers proportionally to the relative dielectric constant and frequency. The conductivity and relative dielectric constant is dominated by fluid saturant compared to the matrix itself. The bulk of relative dielectric constant (ε_r) is roughly equal to porosity and relative dielectric constant of fluid (ε_r). Due to the fluid/saturant is more conductive, the attenuation becomes higher. The geological material mostly have a relative dielectrical constant is about 3–30, and hence the georadar wave velocity is about 0.06–0.175 m/ns, while the air velocity is 299.8 mm/ns.

The relationship between dielectric, permittivity, and conductivity of medium is governed by

$$\varepsilon^* = \varepsilon' + i\left(\varepsilon'' + \sigma_s/\omega\varepsilon_o\right) \tag{6}$$

where ε^* is a complex permittivity, ε'' is an imaginary part of permittivity, and σ_s is static or DC conductivity, while the complex conductivity is

$$\sigma^* = \sigma' + i\sigma'' = j\omega\varepsilon_o\varepsilon^* \tag{7}$$

where ω is angular frequency.

In the porous medium material where water is a saturant, the bulk dielectric constant and porosity (ϕ) is defined as

$$\varepsilon_r = (1 - \phi)\varepsilon_m + \phi\varepsilon_w \tag{8}$$

where ε_m and ε_w are dielectric constant of matrix and water, respectively. By using a simple relation, $V = c/\sqrt{\varepsilon_r}$, for low loss material where c is georadar wave velocity in the air, the velocity of georadar in the medium is defined as

$$V = c/[(1 - \phi)\varepsilon_m + \phi\varepsilon_w] \tag{9}$$

Eq. (9) shows that if velocity can be extracted, then porosity of medium can be predicted or vice versa.

2.2 Configuration and resolution of georadar survey

Effectiveness and recoverable of georadar survey is determined by the configuration of the survey. At least there are two types of acquisition: monostatic mode and bistatic mode. In the monostatic mode, one antenna is used as transmitter and receiver simultaneously. While in the bistatic mode, the receiver and transmitter are separated using different antenna. Based on the target itself, the configuration of data acquisition can be performed using different ways: radar reflection profiling, wide-angle reflection and reflection (WARR) and common midpoint (CMP) sounding, and transillumination or tomography (**Figure 3**).

The vertical resolution of georadar is defined by its frequency or wavelength. Each antenna of georadar is designed for certain frequency range, where the peak energy will be associated in the peak frequency of the signal. Hence the vertical resolution georadar signal is determined by wavelength divide by four ($\lambda/4$). Meanwhile, the horizontal resolution of georadar is controlled mainly by the number of traces/s (or traces/m), the beam width, the radar cross section of the reflector, and the depth where target is located [4]. The conical beam of georadar signal itself is inversely proportional to the square root of attenuation coefficient ($\sqrt{\alpha}$). It means that the horizontal resolution is better in the medium with high attenuation coefficient [5].

2.3 Data processing

Data processing in radargram depends on the objectives; there is no standard processing workflow. However, usually the processing data is done to gain the signal which is attenuated during propagation, removing some noise by filtering, deconvolution, and diffraction reduction through migration process. For certain purposes, sometimes the conversion from time domain needs to be done to get the depth domain; in this case the velocity model is needed.
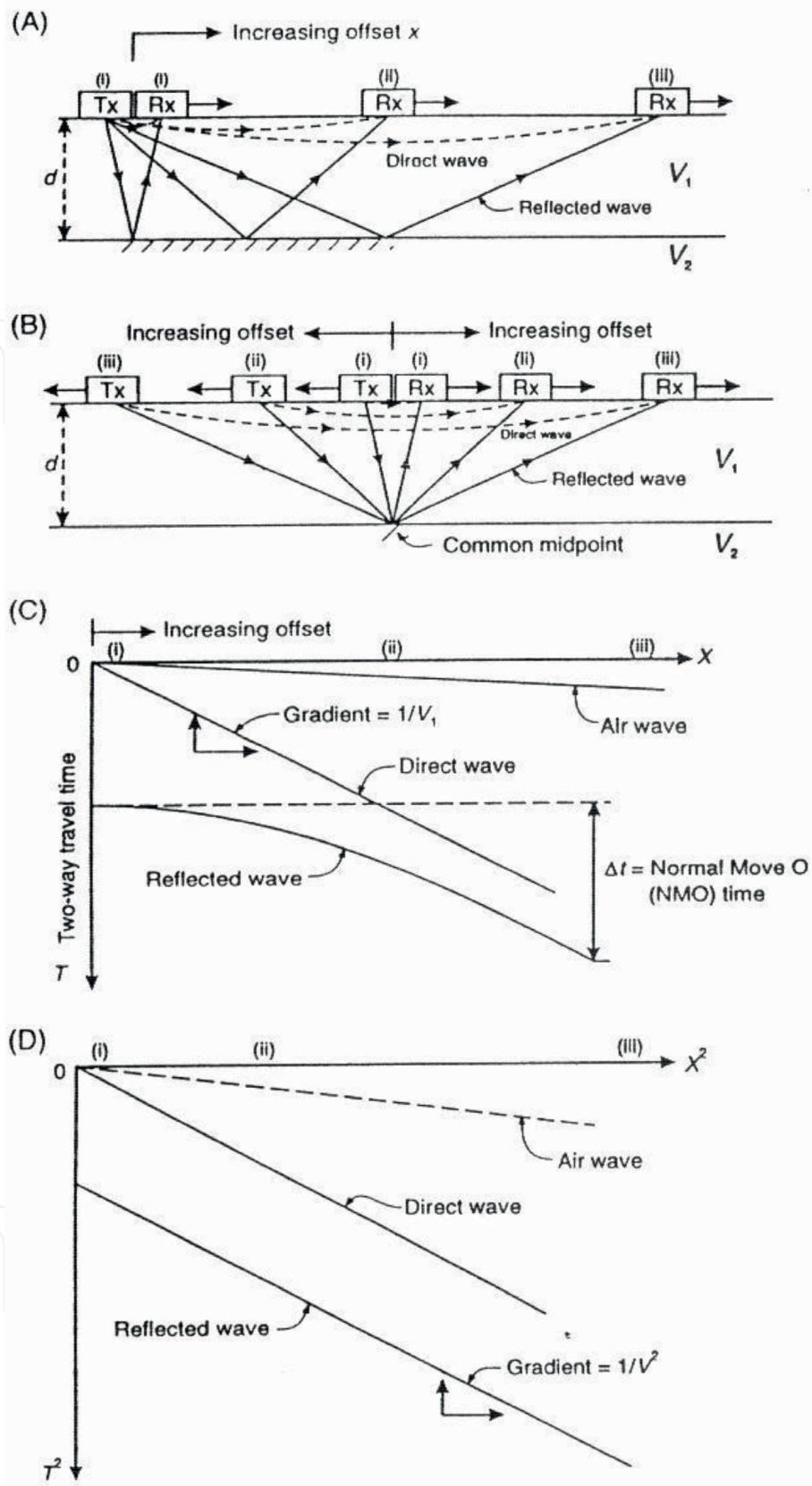
Figure 3.
(A) Sounding WARR dan, (B) sounding CMP, (C) graph of time-offset (T-X) with NMO, (D) graph of relationship T2–X2 [3].

Gain is performed to amplify the amplitude decay due to the distance of propagation. Factors affecting the amplitude decay are attenuation and spherical divergence propagation. Gain is performed by applying a gain function g(t):
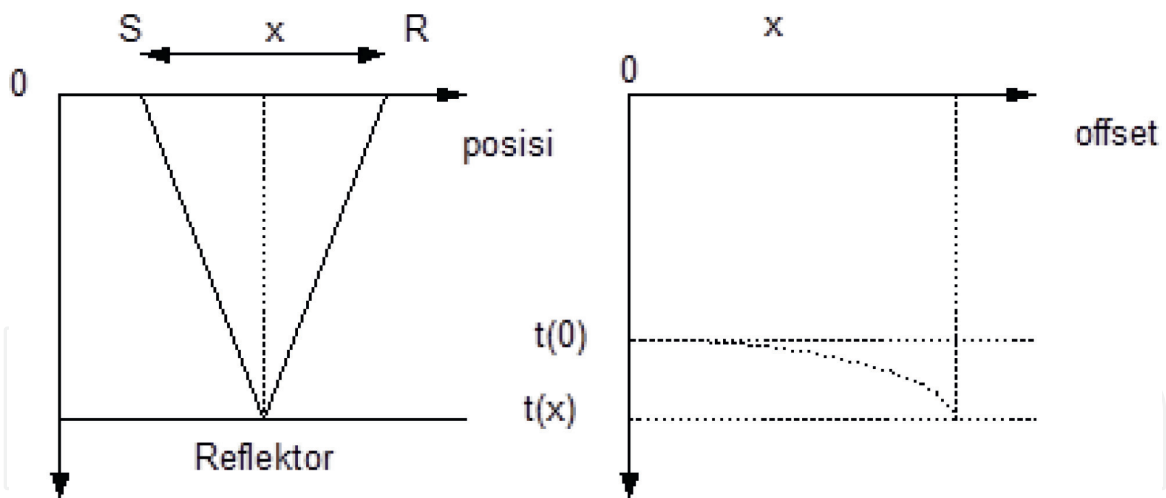
$$\text{Gain (dB)} = A.t + B.20 \, \log(t) + C \tag{10}$$

Figure 4.
Schematic of transmitter and receiver related to the NMO process.

where t is travel time, A is attenuation factor, B is spherical divergence factor, and C is gain constant.

In the implementation on processing, programmed gain control (PGC) and automated gain control (AGC) are commonly used. In the PGC, the gain function is estimated by interpolating the amplitude at certain window sample. While in the AGC, the gain function is generated by taking root mean square (RMS) on each amplitude at certain window. The gain function g(t) is interpolated in the central of the selected window. The window length selection affects the reflector strength in the result. If the window length is too wide, the signal from deeper part will gain less, and if selected window is too small, all the reflection will be gained strongly; in this case it is difficult to distinguish strong reflector from others because all reflector will be gained strongly.

The velocity analysis needs to be conducted to know the value of velocity (velocity model); hence, the true depth and slope can be estimated. Direct measurement of medium velocity can be done from wellbore or indirectly through velocity analysis during normal moveout (NMO) process. The NMO process is illustrated in **Figure 4**:

The function of NMO is describes as follows:

$$T = \frac{2S}{V} = \frac{2\sqrt{\left(\frac{x}{2}\right)^2 + h^2}}{V} \qquad (11)$$

$$T^2 = \frac{4\left(\frac{x^2}{4} + h^2\right)}{V^2} = \frac{x^2}{V^2} + \frac{4h^2}{V^2}, \text{ if } T^2(0) = 4h^2/V^2$$

$$\text{Then } T^2(x) = T^2(0) + \frac{x^2}{V^2}$$

where V is velocity obtained from relation of reflection time at zero offset and offset and distance/offset.

3. Acquisition and processing data

Geological of Bandung area is still young and renewed because of volcanic activities around Bandung area. Based on previous study, there is a Lembang fault in Bandung area which occurred from tectonic process. This fault located in the

southern part of Lembang and crossing Cisarua from east to west of Manglayang mountain. Throw of this fault is varying up to 450 m in Pulasari near to the target area. The Lembang fault was created during the Pleistosen era (about 500,000 years ago) [6].

In the end of Miocene, series of mountains and folds are created in the northern part and in the southern part which become series of volcanos. In the breaking time of Pliocene era, there is no activity of volcanoes and sedimentation, and in the end of Pliocene era, series of mountains were created, and sediments in the northern part were folded and shifted into northern part of Bandung. Materials as a result of volcano eruption activities are distributed into southern part of Bandung.

To detect the existence of Lembang fault, a georadar survey was conducted in this area. Sketch of data gathering in this area is shown in **Figure 5**. The data collection was conducted using common-offset method with 25 and 50 MHz antenna. Most of the profile was selected perpendicular to the fault.

All the data are processed using Seismic Unix (SU) software by performing the scaling on the time sampling rate from nanosecond to millisecond (ms), frequency from megahertz to hertz and velocity from m/ns to m/μs. The details of conversion factor are shown in **Table 1**.

The processing data includes filtering using band-pass filter (10, 20, 30, 50) MHz for antenna 25 MHz and (10, 30, 70, 100) MHz for 50 Hz, AGC, and velocity analysis based on hyperbole fitting curve. The velocity obtained from hyperbole fitting curve is shown in **Table 2**. This velocity model was used to convert time
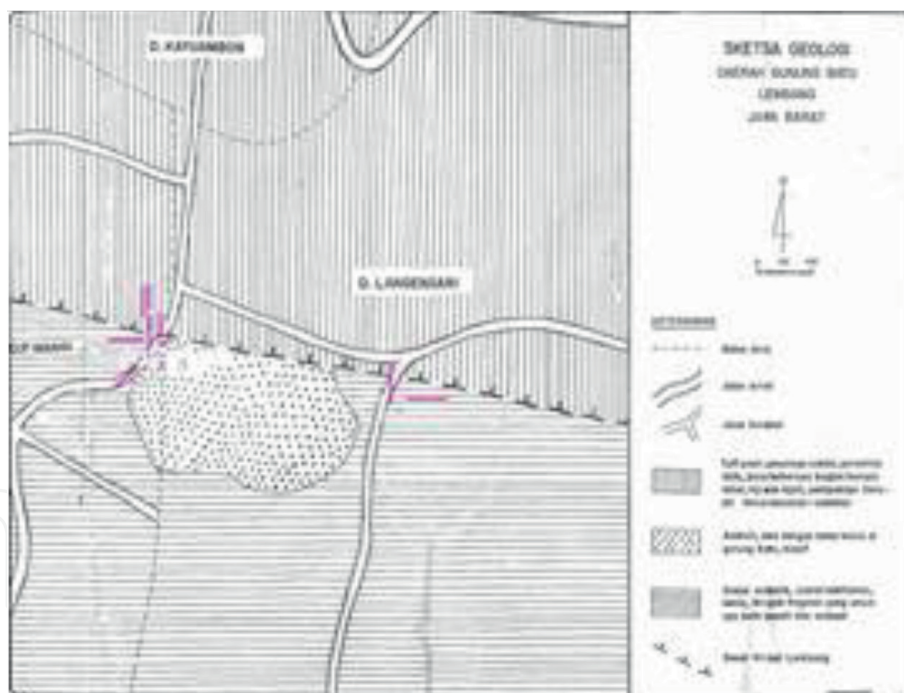

Figure 5.
Georadar data acquisition map.

Parameters	True value	Scaled value
Time sampling rate	1.4 ns	1.4 ms
Nyquist frequency	357 MHz	357 Hz
Offset	1 m	1 m
Radar speed in air	0.3 m/ns	300 m/μ

Table 1.
Conversion from radar into seismic scale.

Depth (m)	Velocity (m/µs)
15.63	196.17
17.16	186.37
22.25	180.69

Table 2.
Velocity model extracted from hyperbole fitting curve during velocity analysis.

domain into depth domain in the profile. In general, the velocity is quite high because the lithology is dominated by tuff, andesite, and breccia volcanic.

4. Result and discussion

Out of several profiles which were studied, profile 03 displayed the large fault in the radargram which is associated with a main Lembang fault. In the other profiles, there are some small fault systems. Based on the velocity analysis, the structure of Lembang fault is a conductive area where the velocity decreases with depth. Profile in **Figure 6** which is taken perpendicular to the fault shows a normal fault system. The foot wall is located in the northern part and hanging wall in the southern part. The position of foot wall part is lower about 7–8 m compared to the hanging wall part. The structure of this area consists of basement which is indicated by a free reflection area and sediment bedding in the horizontal layer. Above the foot wall part, there is a pattern of unconformity.

In **Figure 6**, the top of basement formation is interpreted as the blue line indicates a normal fault. The folded reflection can be resulted as post fault due to the compression from the northern part; the horizontal bedding is folded as small anticline. Cracking in the shoulder of road around this profile indicates that the fault reaches the surface. Those crack lies in the west–east direction where the northern part is lower than southern part. Previous study mentioned that this active
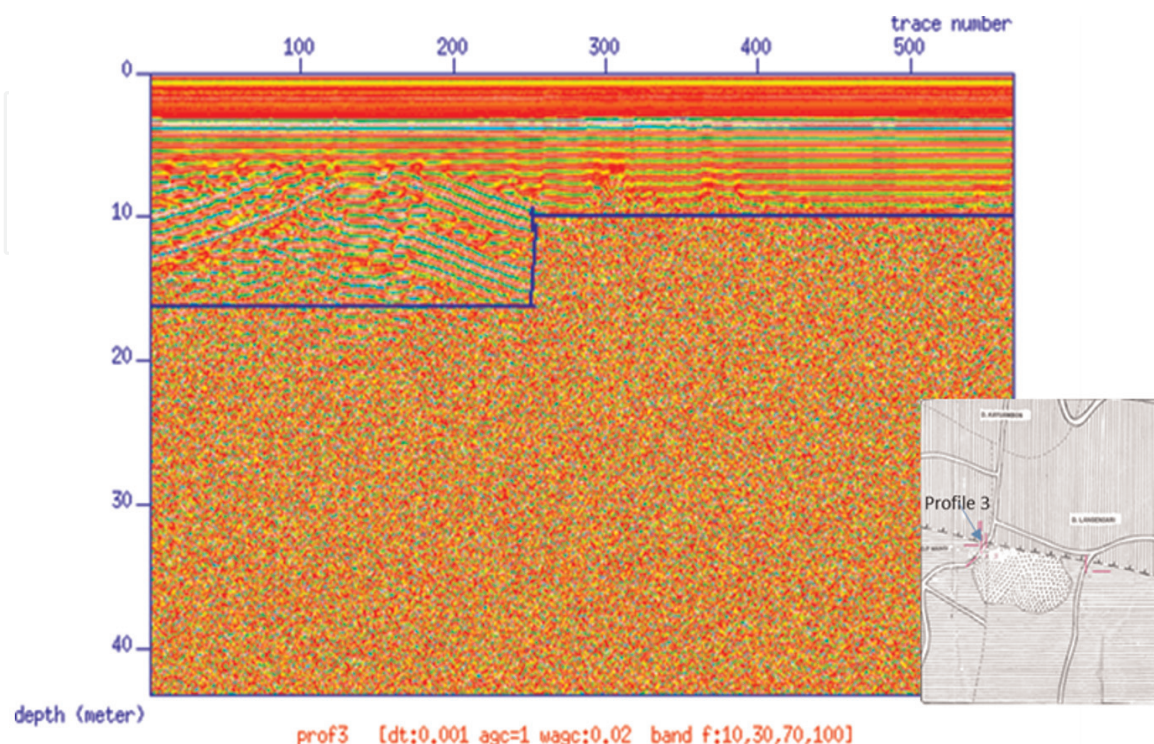

Figure 6.
Cross section taken perpendicular to the fault.

fault has a movement rate per year about 0.3–1.4 cm/year [6]. Instability of this area due to the activities of this fault especially the possible earthquake needs to be monitored further to avoid the further effect like landslide which can damage the urban and suburban area around this fault.
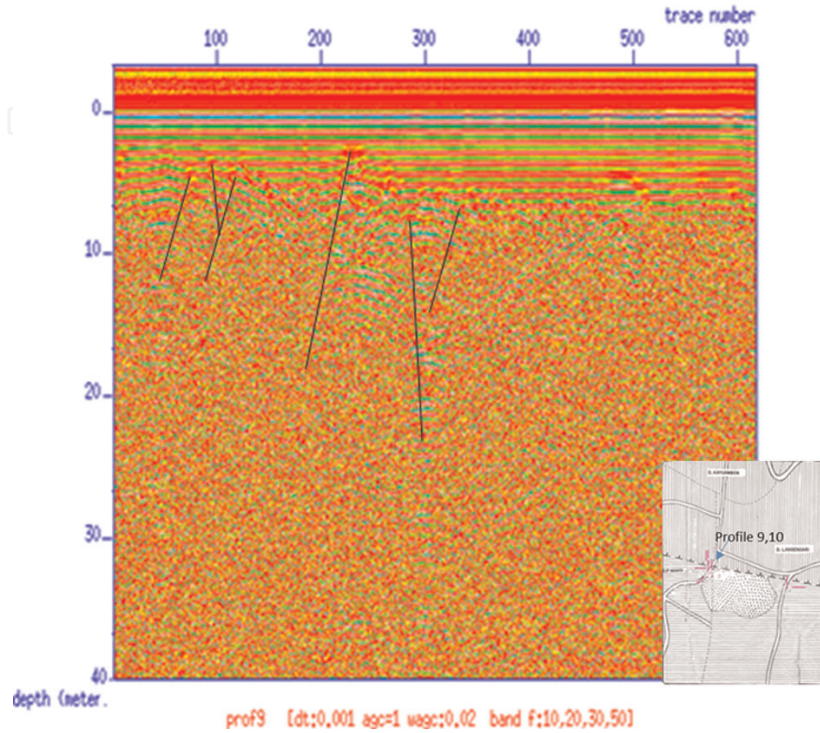

Figure 7.
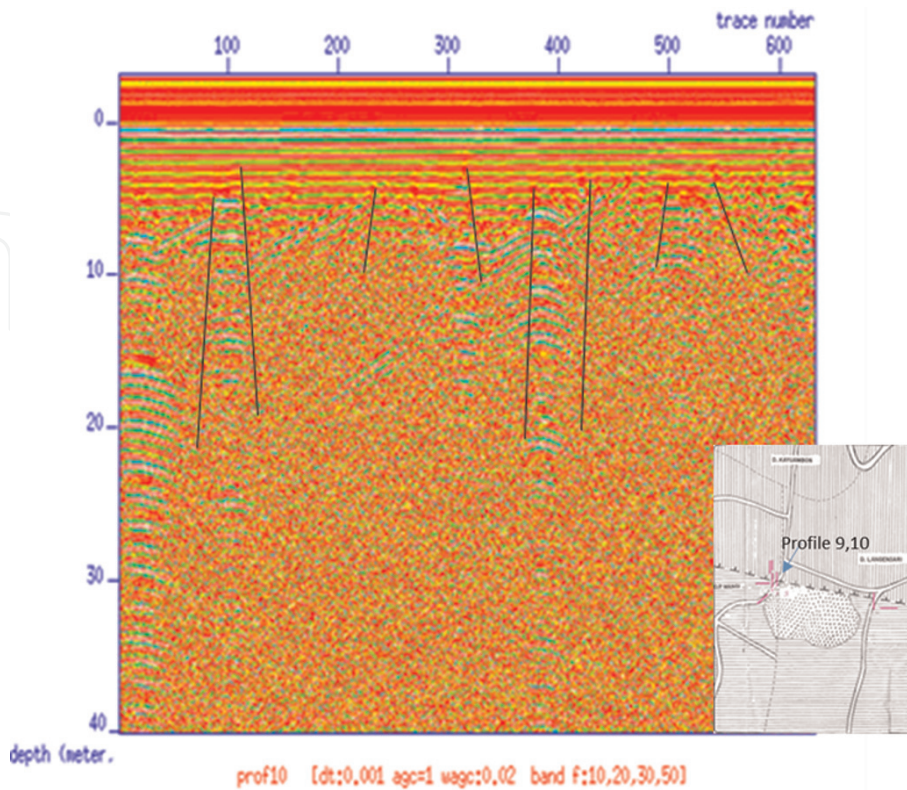*Profile 9 taken perpendicular to the fault line.*

Figure 8.
Profile 10 taken perpendicular to the fault direction.

Small faults around the main fault also recorded in other profiles.
Figures 7 and **8** show the pattern of small fault systems which are still related to the activity of the main fault. Profiles 9 and 10 as shown in **Figures 4** and **5** are taken perpendicular also to the main fault direction. The main fault is not recorded in these profiles. However, the diffraction pattern which indicates small fault system is appearing in this area.

The subduction and compression process in the north–south direction also produces other local fault system. Because the length of this fault is only 29 km, the maximum earthquake due to the energy release in this area is predicted that the earthquake magnitude will not be more than 6 in Richter scale. Tectonic activity record in this area showed that the focus of earthquake is located in the depth of 3–7 km. The earthquake activities are also related to the continuity of three main fault in Bandung area which are Cimandiri fault, Lembang fault, and Baribis fault [6]. Even though the earthquake recorded in this area are not strong earthquakes, because this area is one of the tourism object locations in Bandung and high population around this area, the monitoring of possible hazard needs to be continued. A small earthquake is possible to activate that fault which can trigger instability of the soil mechanism in this area.

5. Conclusion

Lembang fault which is located near the urban area with high population density is successfully imaged using georadar method. Based on radargram result, the foot wall part of Lembang fault is located in the northern part, and hanging wall is located in the southern part. The subsurface structure in this area is dominated by basement and sediment layers. Due to the location of this fault which is near the urban area with high population, further investigation to mitigate the potential of landslide, instability, and activity of this fault needs to be monitored. A CMP survey type can be proposed to be used to improve velocity information; hence, the depth of structure in the subsurface can be improved. A monitoring on the movement of this fault activity using GPS needs to be performed to monitor these activities consciously.

Author details

Maman Hermana[1]*, Maya Genisa[2], Luluan A. Lubis[1] and Chow Weng Sum[1]

1 University Technology of PETRONAS, Perak, Malaysia

2 YARSI University, Jakarta, Indonesia

*Address all correspondence to: maman.hermana@utp.edu.my

IntechOpen

References

[1] Reynolds JM. An Introduction to Applied and Environmental Geophysics. 2nd ed. Wiley-Blackwell; 2011. Retrieved from http://eu.wiley.com/WileyCDA/WileyTitle/productCd-0471485357.html

[2] https://research.lppm.itb.ac.id/2017/07/04/detection-of-burried-bodies-on-landslide-area-using-ground-penetrating-radar-method/

[3] Ramadhan ML, Prawita SM, Fatmasari NW. Identifikasi Bidang Patahan Sesar Lembang dengan Metode Electrical ResistivityTomography untuk Mitigasi Bencana Gempa Bumi dan Longsor. In: Geostone UPN Conference. 2016

[4] Rial FI, Pereira M, Lorenzo H, Arias P, Novo A. Vertical and horizontal resolution of GPR bow-tie antennas. In: Proceedings of the 2007 4th International Workshop on Advanced Ground Penetrating Radar, IWAGPR; July 2007. pp. 187-191. DOI: 10.1109/AGPR.2007.386549

[5] Daniels DJ, Gunton DJ, Scott HF. Introduction to subsurface radar. IEE Proceedings F Communications, Radar and Signal Processing. 1988;**135**(4):278. DOI: 10.1049/ip-f-1.1988.0038

[6] Firdaus MW, Setyawan A, Yusuf M. Gayaberat second vertical gradient studi kasus sesar. Younster Physics Journal. 2016;**5**(1):21-26